RSC Advances

PAPER

View Article Online
View Journal | View Issue

Cite this: *RSC Adv.*, 2025, **15**, 14283

Expansinine, a novel indole alkaloid–ergosteroid conjugate from the endophytic fungus *Penicillium expansum* of *Aconitum carmichaelii*†

Chenzhe Li,[a] Ziruo He,[a] Zhaofei Wen,[a] Guangqian Sun,[a] Xianying Tang,[a] Tianpeng Yin *[b] and Le Cai*[a]

Received 2nd April 2025
Accepted 23rd April 2025

DOI: 10.1039/d5ra02287h

rsc.li/rsc-advances

The endophytic fungus *Penicillium expansum* WTJP1 was isolated from *Aconitum carmichaelii* Debeaux, a famous traditional Chinese medicine known as aconite. Chemical investigation of this aconite-derived fungus led to the isolation of one previously undescribed compound, expansinine (**1**), which represents the first example of an indole alkaloid–ergosteroid conjugate found in nature. The assignments of the structure of **1** were determined by extensive spectroscopic and spectrometric ECD and DP4+ probability analyses. In addition, compound **1** was evaluated for its cytotoxic activities against five human cancer cell lines.

1 Introduction

Indole alkaloids are a class of compounds with a five-membered pyrrole cyclocyclobenzene ring as the common chrematistic skeleton and are often found in fungal secondary metabolites with a wide range of biological activities, such as anti-inflammatory,[1] antitumor,[2] anti-hepatitis,[3] and neuroprotective activities.[4] Due to their diverse chemical structures and pharmacological activities, indole alkaloids are potential sources for novel drug discovery. Thus, investigations of indole alkaloids have shown great value in human society.

Roquefortines are a group of compounds derived from cyclic dipeptides containing an indoline ring that is fused with a diketopiperazine or benzodiazepindinone ring. The most representative compound of the roquefortine family is roquefortine C, which was first isolated from *Penicillium roqueforti* and is often used as a marker to detect the degree of contamination of agricultural products, such as vegetables,[5] cheese,[6] nuts[7] and silage,[8] caused by *Penicillium* strains. This compound has been acknowledged as the precursor of several prenylated indole alkaloids, such as roquefortine E.[9]

Steroids constitute a very large group of natural products that are widely distributed in microbes, animals and plants. The common steroids produced by fungi are ergosteroids, which are remarkable for their diverse biological effects. Because the steroid skeleton is rigid, even a small change in the position of a substituent often results in a large change in biological activity. Thus, it is of great practical significance to explore natural ergosteroids with novel structures.

In our continuing research on the fungal metabolites associated with medicinal *Aconitum* plants,[10] a previously undescribed indole alkaloid–ergosteroid conjugate, expansinine (**1**) (Fig. 1), was isolated from methanol extracts of *Penicillium expansum*, an endophytic fungus of the medicinal plant *Aconitum carmichaelii* Debeaux. The assignments of the structure of **1** were determined by extensive spectroscopic and spectrometric ECD and DP4+ probability analyses. In addition, the cytotoxic activity of this new compound against several common human cancer cell lines was also studied. Herein, the isolation, structural characterization and bioactivities of the new compounds are described, and a biogenetic pathway is proposed.

2 Experimental section

2.1. General experimental procedures and fermentation

NMR spectra were either recorded on a Bruker Avance 400 MHz spectrometer or a Bruker Avance 600 MHz spectrometer

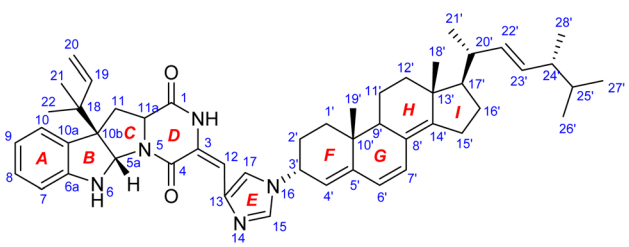

Fig. 1 Structure of expansinine (**1**).

[a]*Key Laboratory of Medicinal Chemistry for Natural Resource, Ministry of Education, Yunnan Characteristic Plant Extraction Laboratory, Institute of International Rivers and Eco-security, School of Chemical Science and Technology, Yunnan University, Kunming 650091, P. R. China. E-mail: caile@ynu.edu.cn*

[b]*School of Bioengineering, Zunyi Medical University, Zhuhai, 519041, China. E-mail: ytp@zmu.edu.cn*

† Electronic supplementary information (ESI) available. See DOI: https://doi.org/10.1039/d5ra02287h

(Bruker, Karlsruhe, Germany) using TMS as the internal reference. HR-ESI-MS data were acquired on an Agilent 1290 UPLC/6545Q-TOF-MS spectrometer. Silica gels (300–400 mesh, Qingdao Haiyang Chemical Co. Ltd., Qingdao, China) and Sephadex LH-20 (Solarbio Science & Technology Co. Ltd, Beijing, China) were used for column chromatography (CC). The CH_2Cl_2, CH_3OH, ethanol, petroleum ether (PE) and ethyl acetate (EA) used for CC were chemically pure. Fractions were monitored by TLC and visualized by spraying with 10% H_2SO_4 in ethanol followed by heating. Potato dextrose agar (PDA) slant culture medium was used to cultivate the strain in a constant-temperature incubator at 28 °C for 6 days. Then, mature *P. expansum* was added to solid-state fermentation culture medium (100 g potato as culture substrate in each bottle) that had been sterilized at 121 °C for 30 min before incubation at 28 °C for 30 days.

2.2. Plant and fungal material

A. carmichaelii was collected from Guiyang City, Guizhou Province, China, in June 2021 and was authenticated by Prof. Yang Chen at Guizhou Medicinal University. The voucher specimen (2021-WT-1) was deposited at the School of Chemical Science and Technology, Yunnan University, China. The *P. expansum* (100% GenBank accession no. MT582774.1) strain, which was isolated from *A. carmichaelii* and cultured on potato dextrose agar (PDA) media, was deposited at the School of Chemical Science and Technology, Yunnan University, China.

2.3. Extraction and isolation

After fermentation, the solid culture was soaked in methanol at room temperature for 24 h and then extracted thoroughly by ultrasonication three times for 30 min. The fermentation products were subsequently decanted, extracted four times with ethyl acetate and concentrated under reduced pressure. The extracts (50.8 g), as dark-brown amorphous solids, were subjected to silica gel CC and eluted with a CH_2Cl_2–CH_3OH gradient system (100 : 0 to 3 : 1) to obtain five fractions. Fr.2 (26.4 g) was chromatographed successively over Sephadex LH-20 (CH_3OH) and silica gel (CH_2Cl_2–CH_3OH, 100 : 1 to 30 : 1) to yield compound **1** (13 mg).

2.3.1. Expansinine (1). Brown, amorphous powder; $[\alpha]_D^{20} = -15.9$ ($c = 0.11$ g·100 ml^{-1}, CH_3OH). IR ν_{max}: 2957, 2931, 1668, 1383 cm^{-1}; HR-ESI-MS at *m*/*z*: 766.5071 $[M + H]^+$ (calcd for $C_{50}H_{64}N_5O_2^+$, 766.5055). The ^{1}H and ^{13}C NMR spectral data are shown in Table 1.

2.4. Cell culture and cytotoxicity MTT assay

Five human cancer cell lines (MCF-7 breast cancer cells, SW480 colon cancer cells, SMMC-7721 hepatocellular carcinoma cells, A549 lung cancer cells, and HL-60 myeloid leukemia cells) were chosen for the cytotoxicity assay, and the *in vitro* cytotoxicity of compound **1** was evaluated *via* the MTS method.[11] Cisplatin (DDP) was used as the positive control. MCF-7, SW480, A549 and HL-60 cells were obtained from the Shanghai Institute of Biochemistry and Cell Biology, Chinese Academy of Sciences

Table 1 ^{1}H (400 MHz) and ^{13}C (100 MHz) NMR spectral data in $CDCl_3$ for compound **1**

No.	δ_H (J in Hz)	δ_C	No.	δ_H (J in Hz)	δ_C
1	—	166.8 s	1′	1.59 m; 1.41 m	29.6 t
2	9.46 brs	—	2′	2.19 m; 1.93 d (14.5)	27.6 t
3	—	123.6 s	3′	4.80 t (4.5)	52.2 d
4	—	158.9 s	4′	5.53 d (4.7)	117.1 d
5	—	—	5′	—	149.6 s
5a	5.63 brs	78.1 d	6′	5.98 d (10.6)	125.0 d
6	4.98 brs	—	7′	6.33 d (9.6)	128.1 d
6a	—	150.4 s	8′	—	124.6 s
7	6.56 d (7.7)	109.1 d	9′	2.16 m	45.2 d
8	7.08 t (7.6)	129.0 d	10′	—	36.0 s
9	6.74 t (7.5)	119.0 d	11′	1.64 m; 1.57 m	19.6 t
10	7.16 d (7.5)	125.3 d	12′	2.06 m; 1.33 m	36.4 t
10a	—	129.1 s	13′	—	43.9 s
10b	—	61.6 s	14′	—	151.3 s
11	2.56 dd (12.3, 5.9); 2.47 m (overlap)	37.0 t	15′	2.38 m; 2.45 m	25.2 t
	2.47, m (overlap)		16′	1.81 m; 1.49 m	28.0 t
11a	4.02 dd (11.3, 5.9)	59.0 d	17′	1.26 m	56.0 d
12	6.63 s	117.8 d	18′	0.95 s	19.3 q
13	—	135.2 s	19′	0.90 s	17.7 q
14	—	—	20′	2.13 m	39.5 d
15	8.31 s	123.3 d	21′	1.05 d (6.6)	21.4 q
16	—	—	22′	5.21 dd (15.2, 7.7)	135.4 d
17	7.56 s	136.5 d	23′	5.26 dd (15.2, 7.1)	132.4 d
18	—	41.1 s	24′	1.88 m	43.0 d
19	5.98 dd (17.2, 10.6)	143.7 d	25′	1.48 m	33.2 d
20	5.11 d (10.8); 5.08, d (17.3), 5.08 d (17.3)	114.6 t	26′	0.84 d (6.8)	20.1 q
21	1.13 s	22.6 q	27′	0.83 d (6.8)	19.8 q
22	1.02 s	23.1 q	28′	0.93 d (6.8)	17.8 q

(Shanghai, China), SMMC-7721 cells were obtained from Beijing Beina Chuanglian Biotech Institute (Beijing, China).

2.5. TDDFT-ECD calculations & NMR computational methods

TDDFT-ECD calculations[12,13] and NMR calculations[14,15] were conducted according to the reference, details see ESI.†

3 Results and discussion

Compound **1** was isolated as a brown powder, and its molecular formula was determined to be $C_{50}H_{63}N_5O_2$ based on HR-ESI-MS at *m*/*z* 766.5071 $[M + H]^+$ (calcd for $C_{50}H_{64}N_5O_2^+$, 766.5055), indicating 22 degrees of unsaturation. The IR spectrum exhibited an absorption peak corresponding to the carbonyl group (1668 cm^{-1}).

The ^1H NMR spectrum of 1 revealed a group of diagnostic signals for a dihydroindole fragment (δ_H 4.98 brs, 5.53 d, 5.63 brs; δ_C 6.75 t, 7.16 d, 7.08 t),[16] which can be further confirmed by consecutive ^1H–^1H COSY correlations from H-7 to H-10 and from H-5a to NH. This dihydroindole fragment (rings A and B) was fused with a tetrahydropyrrole ring (ring C) by sharing the bridging carbons C-5a and C-11 according to the HMBC correlations from H-11 to C-10a and C-5a and from H-11a to C-10b and C-5a (Fig. 1). A common isopentenyl group with a terminal double bond can also be easily identified in its ^1H and ^{13}C NMR spectra (δ_H 1.03 s, 1.14 s, 5.08 d, 5.12 d, 5.99 dd; δ_C 22.6 q, 23.1 q, 41.4 s, 114.6 t, 143.7 d), and this group was connected to the dihydroindole group at C-10b, as revealed by the HMBC correlations from H-21, H-22 and H-10 to C-10b. In addition, an imidazole ring (ring E) was recognized according to the characteristic signals at δ_H 7.56 brs, 8.31 s, and δ_C 123.3 d, 135.2 s, 136.5 d. A trisubstituted double bond was connected to the imidazole ring at C-13, as revealed by the HMBC correlation from H-17 to C-12. Finally, the abovementioned two portions were linked through two amide bonds, forming the six-membered ring D. Thus, a roquefortine-type indole alkaloid portion was established. Moreover, the NMR data of this portion were highly consistent with those of roquefortine C (Fig. 2), which further supports the presence of the roquefortine C segment in the molecule as deduced.

The ^{13}C and DEPT spectra revealed that the remaining 28 carbons included six methyl groups, six methylene groups, eleven methine groups, and five quaternary carbons. Among them, four double bonds (δ_C 117.1 d, 149.6 s, 125.0 d, 128.1 d, 124.6 s, 151.3 s, 135.4 d, and 132.4 d) were identified. The data summarized, in combination with the above identified structure, indicated a tetracyclic framework for the other portion of 1. The ^1H NMR spectrum exhibited concentrated high-field signals at δ_H 0.8–2.5, including six methyl signals (δ_H 0.91 s, 0.95 s, 1.05 d, 0.95 d, 0.85 d, 0.83 d), implying the presence of an ergosterol-type sterol for 1. Careful comparison of the NMR data with those of (22*E*,24*R*)-3α-ureidoergosta-4,6,8(14),22-tetraene[17] suggested that they possess identical structures except for the substituent at C-3. Thus, the other portion of compound **1** was established. These two portions were connected through a C-3′-N-16 bond, as revealed by the HMBC correlations from H-3′ to C-15 and C-17. Therefore, the planar structure of **1** was determined as shown in Fig. 1.

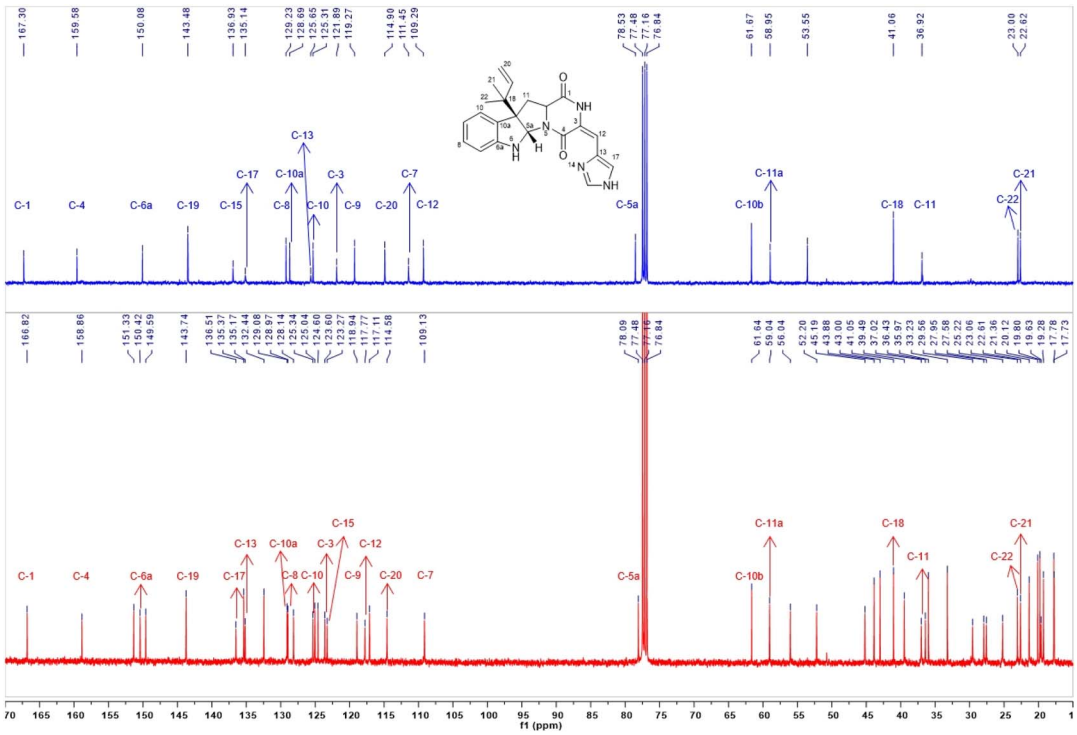

Fig. 2 ^{13}C-NMR spectra of 1 (below) and roquefortine C (above) ($CDCl_3$, 400 MHz).

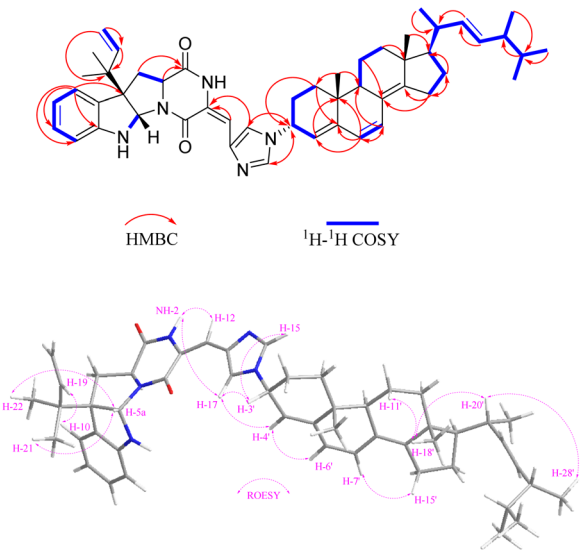

Fig. 3 Key H–^{1}H COSY, HMBC, and NOE correlations of **1**.

The relative configuration of **1** was deduced on the basis of the NOESY correlations along with the vicinal coupling constants (Fig. 3). NOESY correlations between NH-2 (δ_H 9.46 brs) and H-12 (δ_H 6.63 s) suggested an *E*-oriented configuration for $\triangle^{3,12}$. Additionally, the NOESY correlations between H-5a (δ_H 5.63 brs) and H-21 (δ_H 1.14 s), as well as those between H-5a and H-22 (δ_H 1.02 s), indicated that H-5a and the isopentenyl group are oriented in the same direction within the molecular plane. Hence, the configuration of the indole alkaloid fragment was confirmed to be identical to that of the reported compound roquefortine C, *i.e.*, C-10b is in the *R*-configuration while C-5a and C11a are in the *S*-configuration. The 15.2 Hz coupling constant of $\triangle^{22',23'}$ revealed its *E*-oriented configuration, and the stereochemistry of *R*-oriented configured C24′ was determined by comparing the chemical shifts of the compound with those of the ref. 18. According to the literature, the absolute configurations of C-9′, C-10′, C-13′, C-17′, C-20′ and C-24′ are in the *R*-configuration due to they shared the same biogenetic pathway of forming ergosterol.[19] The signal at δ_H 4.80 was assigned to H-3′ as α-oriented because H-3′ is a triple peak with a coupling constant of 4.9 Hz, unlike β-oriented H-3′, which often shows the shape of ddd peaks.[20]

To further determine the relative configuration of 1, the calculated ECD curves performed by TDDFT calculation at the CAM-B3LYP/6-311+G(d,p) level of 1a and 1b were compared with the experimental curve, and the results showed that the curve of 1a better matched the experimental data (Fig. 4). Moreover, **1a** and **1b** were subjected to NMR chemical shift calculations using the gauge independent atomic orbital (GIAO) method[14] at the PCM/mPW1PW91/6-311+G(d,p) level. According to the results, all the data (^{1}H + ^{13}C) of DP4+ unambiguously supported **1a** as the most likely isomers at 100.00% (Fig. 5). Thus, the absolute configuration of **1** was confirmed. To be 5a*S*, 10b*R*, 11a*S*, 3′*R*, 9′*R*, 10′*R*, 13′*R*, 17′*R*, 20′*R*, 24′*R*.

Compound **1** is the first example of a conjugate of an indole alkaloid and an ergosteroid. Based on its molecular

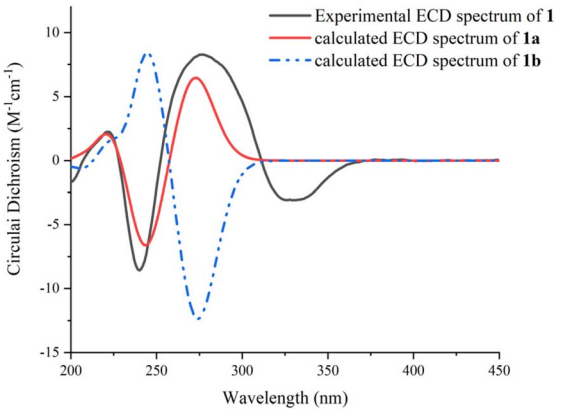

Fig. 4 Experimental and calculated ECD spectra of compound **1**.

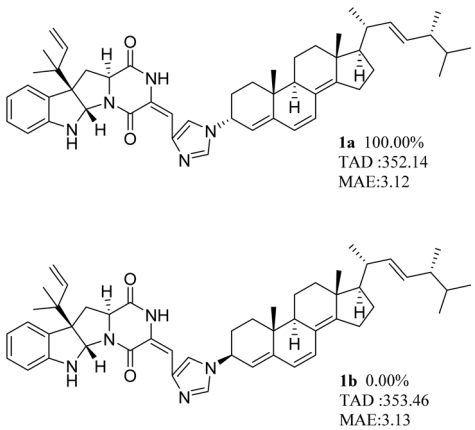

Fig. 5 Total absolute deviation (TAD), mean absolute error (MAE), and DP4+ probability analyses for expansinine (**1**).

architecture, two important biogenetic precursors were deduced to be roquefortine C (**2**) and ergosta-4,6,8(14),22-tetraen-3-one (**3**), while the former compound was also isolated in this study. Roquefortine C is a typical prenylated indole alkaloid with a cyclic dipeptide framework that is biosynthesized from L-tryptophan and L-histidine. HTD has been identified as an important intermediate in its biosynthetic pathway.[9] After reversed prenylation and ring closure of HTD catalyzed by DMAPP, roquefortine C might be formed through two possible branches of the roquefortine pathway as shown in Fig. 6.[21] Another biogenetic precursor 3 is formed by dehydrogenation of ergosterol,[22] a common fungal metabolite that is biosynthesized mainly *via* the mevalonate (MVA), farnesyl pyrophosphate (FPP) and ergosterol pathways.[19] Finally, a reductive amination reaction between these two precursors led to the formation of the indole alkaloid–ergosteroid conjugate, which could be catalyzed by amine dehydrogenases with high enantioselectivity.[23]

Compound **1** was evaluated for its *in vitro* cytotoxic activities against five common human cancer cell lines, HL-60, A549, SMMC-7721, MDA-MB-231, and SW480. Unfortunately, compound **1** exhibited no cytotoxic activity at a concentration of 40 μM.

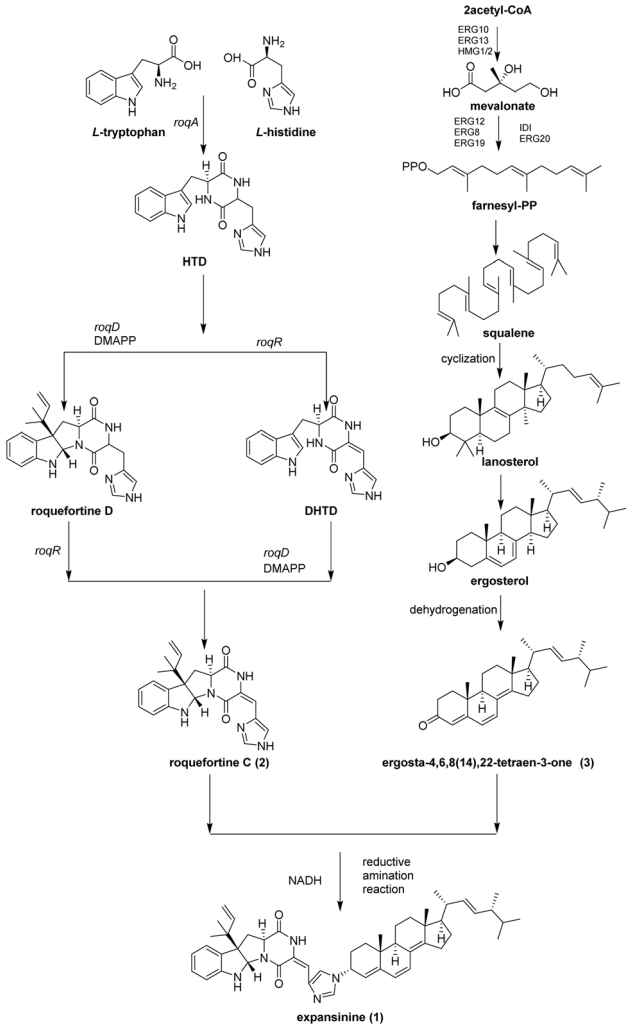

Fig. 6 Proposed biosynthetic pathway for expansinine (**1**).

4 Conclusions

In summary, expansinine (**1**), a previously undescribed type of C_{50} secondary metabolite formed by connection of a roquefortine-type indole alkaloid with an ergosteroid, was isolated from *P. expansum*, an endophytic fungus of the medicinal plant *A. carmichaelii*. This is the first example of an indole alkaloid–ergosteroid conjugate found in nature. The structure and configurations were elucidated on the basis of HR-ESI-MS, IR, 1D, and 2D NMR. Compound 1 did not exhibit potential inhibitory effects on HL-60, A549, SMMC-7721, MDA-MB-231, or SW480 cells *in vitro*.

Data availability

The data supporting this article have been included as part of the ESI.†

Author contributions

Chen-Zhe Li: investigation, writing – original draft, writing – review & editing. Zi-Ruo He: visualization. Zhao-Fei Wen: validation. Guang-Qian Sun: investigation. Xian-Ying Tang: data curation. Tian-Peng Yin: visualization, supervision, funding acquisition. Le Cai: Resources, conceptualization, supervision, funding acquisition.

Conflicts of interest

There are no conflicts to declare.

Acknowledgements

This project was supported by a grant from the Guizhou Provincial Basic Research Program (Natural Science) (No. QKHJC-ZK[2024]YB263) and a grant from the Zhuhai Basic and Applied Basic Research Foundation (No. 2220004002942), a grant from the Science and Technology Innovation Team of Zhuhai Campus of Zunyi Medical University (ZHTD2024-2), the Project of Yunnan University "Double First Class" Construction Joint Project (202201BF070001-014); the Project of Yunnan Characteristic Plant Screening and R&D Service CXO Platform (2022YKZY001); Yunnan University's Research Innovation Fund for Graduate Students (ZC-24249896).

References

1 Y. H. Zhang, H. F. Du, Y. F. Liu, F. Cao, D. Q. Luo and C. Y. Wang, *Appl. Microbiol. Biotechnol.*, 2024, **108**, 194.
2 M. Asano, K. Harada, T. Yoshikawa, T. Bamba and K. Hirata, *Biosci., Biotechnol., Biochem.*, 2010, **74**, 386–389.
3 F. Ni, S. Kota, V. Takahashi, A. D. Strosberg and J. K. Snyder, *Bioorg. Med. Chem. Lett.*, 2011, **21**, 2198–2202.
4 Y. J. Li, J. Li, L. Xie, J. Y. Zhou, Q. X. Li, R. Y. Yang, Y. P. Liu and Y. H. Fu, *Nat. Prod. Res.*, 2022, **36**, 5181–5188.
5 Z. Maskova, Z. Barboráková, K. Pilarčíková, M. Mrvová and D. Tančinová, *J. Microbiol., Biotechnol. Food*, 2023, **12**, e9925.
6 S. Ozturkoglu-Budak, H. C. Akal and H. I. Öztürk, *World Mycotoxin J.*, 2023, **16**, 273–283.
7 P. Rodrigues, A. Jelassi, E. Kanoun, M. Sulyok, P. Correia, E. Ramalhosa and E. L. Pereira, *J. Food Sci.*, 2023, **88**, 848–859.
8 T. J. Snelling, D. R. Davies, J. A. Huntington, N. Adams, H. Warren, J. Taylor-Pickard and L. A. Sinclair, *Front. Agron.*, 2023, **5**, 1146505.
9 S. Ohmomo, T. Sato, T. Utagawa and M. Abe, *Agric. Biol. Chem.*, 1975, **39**, 1333–1334.
10 Y. T. Shao, H. Yan, T. P. Yin, Z. W. Sun, H. D. Xie, L. D. Song, K. C. Sun and W. Li, *J. Antibiot.*, 2020, **73**, 77–81.
11 N. Zhang, Y. L. Chen, R. X. Jiang, E. W. Li, X. L. Chen, Z. J. Xi, Y. L. Guo, X. Z. Liu, Y. G. Zhou, Y. S. Che and X. J. Jiang, *Autophagy*, 2011, **7**, 598–612.
12 D. Gan, L. Zhu, X. R. Zhang, C. Z. Li, C. Y. Wang, L. Cai and Z. T. Ding, *Org. Chem. Front.*, 2022, **9**, 2405–2411.
13 Y. Shu, J. P. Wang, B. X. Li, J. L. Gan, H. Ding, R. Liu, L. Cai and Z. T. Ding, *Phytochem.*, 2022, **194**, 113009.
14 N. Grimblat, M. M. Zanardi and A. M. Sarotti, *J. Org. Chem.*, 2015, **80**, 12526–12534.

15 C. Y. Wang, D. Gan, Y. Shu, R. F. Mei, J. Q. Liu, C. Z. Li, L. Cai, S. Q. Zhang, L. Zhu, H. Zhou, L. Cai and Z. T. Ding, *Phytochem.*, 2024, **228**, 114251.
16 M. S. Volkova, A. M. Efremov, E. N. Bezsonova, M. D. Tsymliakov, A. I. Maksutova, M. A. Salykina, S. E. Sosonyuk, E. F. Shevtsova and N. A. Lozinskaya, *Molecules*, 2022, **27**, 7462.
17 K. Yoshikawa, M. Ikuta, S. Arihara, E. Matsumura and S. Katayama, *Chem. Pharm. Bull.*, 2001, **49**, 1030–1032.
18 A. M. Metwaly, H. A. Kadry, A. A. El-Hela, A.-E. I. Mohammad, G. Ma, S. J. Cutler and S. A. Ross, *Phytochem. Lett.*, 2014, **7**, 1–5.
19 Y. Q. Jiang and J. P. Lin, *World J. Microbiol. Biotechnol.*, 2022, **38**, 93.
20 Z. J. Pang and O. Sterner, *Nat. Prod. Lett.*, 1993, **3**, 193–196.
21 H. Ali, M. I. Ries, J. G. Nijland, P. P. Lankhorst, T. Hankemeier, R. A. L. Bovenberg, R. J. Vreeken and A. J. M. Driessen, *PLoS One*, 2013, **8**, e65328.
22 J. D. White and S. I. Taylor, *J. Am. Chem. Soc.*, 1970, **92**, 5811–5813.
23 H. Huo, G. Yao and S. Wang, *Catalysts*, 2020, **10**, 1451.